Journal of Engineering and Applied Sciences 12 (5): 1140-1146, 2017
ISSN: 1816-949X

In Silico Determination and Validation of FhuE Structure and Ligand Binding Site as a Vaccine Candidate in *Acinetobacter Baumannii*

Bahare Baharie, Fateme Sefid, Reihane Ragheb, Vahide Saeidjavan,
Hamed Karamizade, Sepide Akhgari and Nazgol Emamian
Departeman of Biology, Science and Art University, Yazd, Iran

Abstract: *Acinetobacter baumannii* is a gram-negative bacterium that causes serious infections in compromised patients. This pathogen grows under a wide range of conditions including iron-limiting conditions. Multidrug resistant *Acinetobacter baumannii* is recognized to be among the most difficult antimicrobial-resistant gram negative bacilli to control and treat. One of the major challenges that the pathogenic bacteria face in their host is the scarcity of freely available iron. To survive in such conditions, bacteria express new proteins in their outer membrane and also secrete iron chelators called siderophores. In the case of human hosts, the free iron availability is 10^{-18} M which is far less than what is needed for the survival of the invading bacterial pathogen. To survive in such conditions, *Acinetobacter baumannii* expresses fhue in its outer membrane. Evidence suggests that fhue iron uptake protein is a useful antigen for inclusion in an effective vaccine, hence the identification of its structure is very important.

Key words: *Acinetobacter baumannii*, fhuE, 3D structure, uptake protein, bacteriostatic

INTRODUCTION

Acinetobacter baumannii is a gram-negative opportunistic pathogen that causes nosocomial infections such as pneumonia, urinary tract infection, bacteremia, meningitis and wound infection (Eliopoulos *et al*., 2008). The bacteria cause illness mostly in patients hospitalized in an Intensive Care Unit (ICU) or with a compromised immune system (Peleg *et al*., 2008). Additionally this bacterium is emerging as multi-or pandrug-resistant which makes treatment much more difficult (Dijkshoorn *et al*., 2007; Valencia *et al*., 2009; Aydin *et al*., 2013). Thus, the rate of mortality is relatively high and alternative therapeutic targets seem to be necessary to combat the bacterium (Gaddy *et al*., 2012).

Iron is an essential micronutrient for all living organisms. All aerobic and anaerobic bacteria, except for Lactobacillus and the causative agent of Lyme disease, need iron for survival (Andrews *et al*., 2003). Iron, functioning as a cofactor, has a significant role in the key metabolic processes and pathogenesis of bacteria (Ratledge and Dover, 2000). In mammals, free iron binds to carrier proteins such as lactoferrin and transferrin (Skaar, 2010) and thus the iron needed for bacterial pathogenesis is restricted. This is considered to be a protective mechanism against bacterial pathogenesis (Ganz, 2009). Bacteria have developed alternative mechanisms for iron uptake to overcome this limitation. One of the most important mechanisms is synthesis and secretion of siderophores. Siderophores have a low molecular weight and a high affinity to Fe (III) (Ong *et al*., 2006; Sandrini *et al*., 2010; Krewulak and Vogel 2008).

Consequently, Iron-Regulated Outer Membrane Proteins (IROMPs) are expressed on the bacterial surface to uptake the ferricsiderophore complex (Santander *et al*., 2012). For *A. baumannii*, iron uptake is one of the processes known to play a key role in infection and establishment in the host (Vallenet *et al*., 2008). Acinetobactin, a catecholate iderophore composed of equimolar quantities of 2,3-dihydroxybenzoic acid, L-threonine and N-hydroxy histamine, is secreted for iron chelating in *A. baumannii* (Mihara *et al*., 2004; Zimbler *et al*., 2009).

Fhue is one of the most important outer membrane protein in pathogenic Acinetobacter species and especially *Acinetobacter baumannii*, belonging to the Ton B-dependent transporter protein family and it is expressed under iron-limited conditions (Zimbler *et al*., 2013). New genome analysis tools based on bioinformatics and immunoinformatics approaches help us select suitable antigens or epitopes directly from the genomes of pathogens in order to design a vaccine. These tools could be employed for epitope selection and vaccine design. Moreover, prediction of protein structures is one of their wide applications (Kafee and Sefid; Payandeh *et al*., 2015; Sefid *et al*., 2016;

Corresponding Author: Fateme Sefid, Departeman of biology, Science and Art University, Yazd, Iran

Dehghani and Sefid, 2016; Darbandian and Sefid, 2017; Sefid *et al*., 2013; Sefid *et al*., 2015; Sefid *et al*., 2016; Kafee and Sefid, 2016; Masoumi and Sefid, 2016). Evidence suggests that Fhue protein is a useful antigen for inclusion in an effective vaccine, hence the identification of its structure is very important. The present study was designed to in silico resolving the major obstacles in the control or in prevention of the *Acinetobacter baumannii* disease. We exploited bioinformatic tools to better understanding and characterizing the fhue structure.

MATERIALS AND METHODS

Sequence availability and homology search: The fhuE protein sequence with accession KMV27515.1 and GI 885078824 acquired from NCBI at http://www.ncbi.nlm.nih.gov/protein was saved in FASTA format for further analyses. The sequences served as a query for protein BLAST at http://blast.ncbi.nlm.nih.gov/Blast.cgi against non redundant protein database. Probable putative conserved domains of the query protein were also searched for at the above address.

Primary sequence analysis: Protparam online software at http://expasy.org/tools/protparam.html was employed for estimation and determination of properties such as molecular weight, theoretical pI, amino acid composition, total number of negatively and positively charged residues, instability index and aliphatic index.

3d structure prediction: The SWISS-MODEL workspace at http://swissmodel.expasy.org/ is a web-based integrated service dedicated to protein structure homology modelling. It assists and guides the user in building protein homology models at different levels of complexity. Building a homology model comprises four main steps: identification of structural template(s), alignment of target sequence and template structure(s), model building and model quality evaluation. These steps can be repeated until a satisfying modelling result is achieved. Each of the four steps requires specialized software and access to up-to-date protein sequence and structure databases.

Ligand binding site predictions: Cofactor at http://zhanglab.ccmb.med.umich.edu/COFACTOR/is a structure-based method for biological function annotation of protein molecules. Important amino acid involved in ligand binding site is predicted by this server.

Pocket detection: Dog site scorer at http://dogsite.zbh.uni-hamburg.de/is an automated pocket detection and analysis tool which can be used for protein drugability assessment. Predictions with Do G site scorer are based on calculated size, shape and chemical features of automatically predicted pockets, incor fhu eted into a support vector machine for druggability estimation.

Identification of functionally and structurallyimportant residues: Inter pro surf at http://curie.utmb.edu/pattest 9.html predicting functional sites on protein surface using patch analysis was employed. Fhu E 3D structure, served as an input file for this server.

RESULTS AND DISCUSSION

Sequence availability and homology search: The protein sequence with 718 residues obtained from NCBI and saved in FASTA format. Protein sequence serving as query for BLAST produced a set of sequences as the highest similar sequence.

BLAST search revealed numerous hits to the FhuE subunit sequence. All hits were of *Acinetobacter baumannii*. Putative conserved domains were detected within this sequence and are shown in Fig. 1. TonB dependent/ligand-gated channels are created by a monomeric 22 strand (22, 24) anti-parallel beta-barrel. Ligands apparently bind to the large extracellular loops. The N-terminal 150-200 residues form a plug from the periplasmic end of barrel. Energy (proton-motive force) and tonB-dependent conformational alteration of channel (parts of plug and Loops 7 and 8) allow passage of ligand. FepA residues 12-18 form the tonB box which mediates the interaction with the ton B-containing inner membrane complex. TonB preferentially interacts with ligand-bound receptors. Transport thru the channel may resemble passage thru an air lock. In this model, ligand binding leads to closure of the extracellular end of pore Then, a TonB-mediated signal facillitates opening of the interior side of pore deforming the N-terminal plug and allowing passage of the ligand to the periplasm. Such a mechanism would prevent the free diffusion of small molecules thru the pore. TonB-dependent siderophore receptor This subfamily model encompasses a wide variety of ton B-dependent outer membrane siderophore receptors. It has no overlap with tonB receptors known to transport other substances but is likely incomplete due to lack of characterizations.

Primary sequence analysis: The protein sequence served as input for the computation of various physical and chemical parameters. The computed parameters included the molecular weight, theoretical pI, instability index, aliphatic index and grand average of hydropathicity

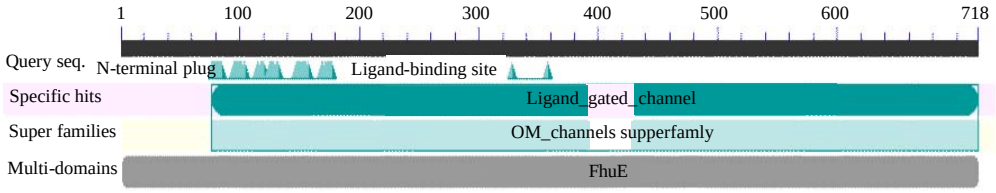

Fig. 1: Putative conserved domains have been detected

(indicates the solubility of the proteins: positive GRAVY (hydrophobic), negative GRAVY (hydrophilic)) are summarized:

- Number of amino acids = 718
- Molecular weight = 79586.3
- Theoretical pI = 5.13

Amino acid composition:

- Ala (A) (57) = 7.9%; Leu (L) (55) = 7.7%
- Arg (R) (24) = 3.3%; Lys (K) (39) = 5.4%
- Asn (N) (52) = 7.2%; Met (M) (10) = 1.4%
- Asp (D) (40) = 5.6%; Phe (F) (26) = 3.6%
- Cys (C) (0) = 0.0%; Pro (P) (25) = 3.5%
- Gln (Q) (35) = 4.9%; Ser (S) (58) = 8.1%
- Glu (E) (39) = 5.4%; Thr (T) (57) = 7.9%
- Gly (G) (58) = 8.1%; Trp (W) (14) = 1.9%
- His (H) (7) = 1.0%; Tyr (Y) (42) = 5.8%
- Ile (I) (320 = 4.5%; Val (V) (48) = 6.7%

Total number of negatively charged residues (Asp+Glu) = 79; total number of positively charged residues (Arg+Lys) = 63

Atomic composition:

- Carbon (C) = 3550
- Hydrogen (H) = 5426
- Nitrogen (N) = 944
- Oxygen (O) = 1121
- Sulfur (S) = 10

Formula:

$$C_{3550}H_{5426}N_{944}O_{1121}S_{10}$$

Total number of atoms = 11051.

Extinction coefficients: Extinction coefficients are in units of M^{-1} cm^{-1}, at 280 nm measured in water; ext. coefficient 139580; abs 0.1% (= g L^{-1}) 1.754.

Estimated half-life: The N-terminal of the sequence considered is M (met). The estimated half-life is: 30 h (*Mammalian reticulocytes*, *in vitro*) >20 h (yeast, *in vivo*) >10 h (escherichia coli, *in vivo*).

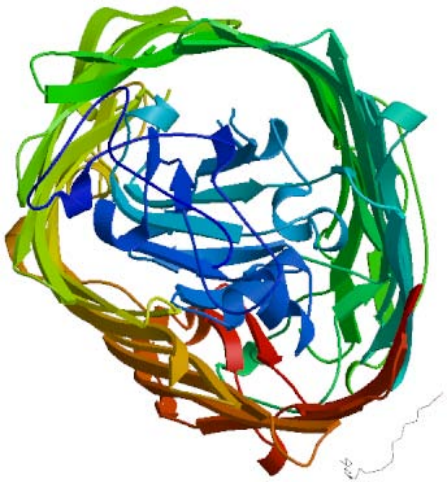

Fig. 2: 3D structure of FhuE

Instability index: The instability index (2) is computed to be 33.62; This classifies the protein as stable. Aliphatic index = 74.58; Grand average of hydropathicity (GRAVY) = -0.461.

3D structure prediction: Building a homology model comprises four main steps: identification of structural template(s) alignment of target sequence and template structure(s) model building and model quality evaluation. These steps can be repeated until a satisfying modelling result is achieved. Each of the four steps requires specialized software and access to up-to-date protein sequence and structure databases. Swiss model software recruited for homology modeling introduced 1 model. Predicted model is shown in Fig. 2.

Ligand binding site predictions: Ligand binding sites determined using COFACTOR software, indicate involvement of conserved residues include 4, 101, 105, 107, 109, 114, 691, 692 in binding site with the highest $cscore^{LB}$ (the confidence score of predicted binding site) (Fig. 3).

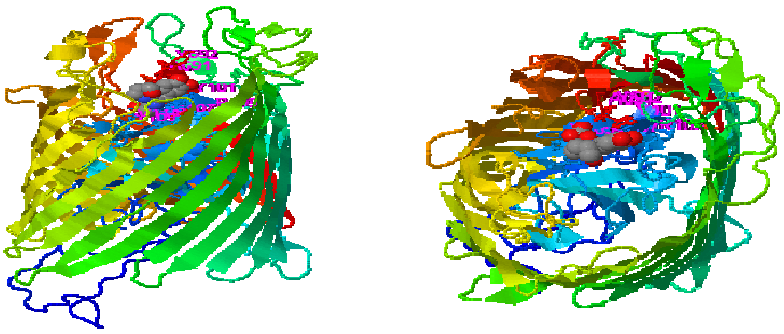

Fig. 3: FhuE ligand binding site predictions

Name	Volume [Å³]	Surface [Å²]	Lipo surface [Å²]	Depth [Å]	Drug Score
P0	3137.28	3258.49	1848.48	40.45	0.80
P1	1547.00	1659.42	1072.25	22.55	0.81
P2	1048.57	1062.82	632.71	33.54	0.81
P3	911.62	1015.39	521.76	23.19	0.83
P4	518.52	515.73	368.44	18.56	0.80
P5	417.98	705.56	443.13	16.40	0.72
P6	373.53	457.80	342.16	13.32	0.62
P7	302.66	533.94	383.39	12.94	0.56
P8	288.54	550.90	355.91	12.70	0.55
P9	250.71	325.99	240.00	14.75	0.60
P10	250.19	251.97	158.53	12.61	0.49
P11	221.04	521.66	272.20	12.14	0.46
P12	217.54	402.62	326.79	10.25	0.41
P13	205.62	383.22	198.35	10.86	0.41
P14	203.16	272.99	132.73	14.86	0.56
P15	188.00	346.42	201.69	13.44	0.49
P16	180.09	399.93	204.73	13.46	0.43
P17	151.85	334.36	301.58	11.28	0.39
P18	150.29	296.67	222.17	10.69	0.37
P19	133.58	312.95	182.60	7.90	0.21
P20	132.42	202.18	103.48	10.55	0.31
P21	125.94	266.48	157.35	7.98	0.20
P22	125.55	247.91	119.00	7.44	0.17
P23	116.09	155.01	105.76	10.65	0.33
P24	112.72	207.42	142.70	7.32	0.18
P25	107.93	203.16	135.75	7.79	0.19

Fig. 4: Pocket descriptor

The calculated BS-score for this predicted binding site was 1.12. BS-score is a measure of local similarity (sequence and structure) between template binding site and predicted binding site in the query structure. Based on large scale benchmarking analysis, observed that a BS-score >1 reflects a significant local match between the predicted and template binding site. Template proteins with similar binding site are listed in Table 1.

Pocket detection: Pockets and descriptors have been calculated for fhuE structure with Do G site scorer: Active site prediction and analysis serveris sumerized in Fig. 4 and 5.

Identification of functionally and structurally important rsidues: Interprosurf annotated functional residues on the 3D structure of fhu E. Residues predicted by auto patch analysis are: 436, 437, 438 438, 456, 457, 477 (Fig. 6).

Table 1: Template proteins with similar binding site

Rank	$Cscore^{LB}$	PDB Hit	TM-score	$RMSD^{a}$	$IDEN^{a}$	Cov.	BS-score	Lig. name	Predicted binding site residues
1	0.37	2w16B	0.930	1.17	0.340	0.942	1.12	PVE	101,105,107,109,114,691,692
2	0.04	1nqgA	0.721	2.94	0.161	0.776	0.71	CA	653,655,657,684,685

$Cscore^{LB}$ is the confidence score of predicted binding site; CscoreLB values range in between (0-1) where a higher score indicates a more reliable ligand-binding site prediction; BS-score is a measure of local similarity (sequence and structure) between template binding site and predicted binding site in the query structure; Based on large scale benchmarking analysis, we have observed that a BS-score >1 reflects a significant local match between the predicted and template binding site; TM-score is a measure of global structural similarity between query and template protein; RMSDa the RMSD between residues that are structurally aligned by TM-align; IDENa is the percentage sequence identity in the structurally aligned region; Cov. represents the coverage of global structural alignment and is equal to the number of structurally aligned residues divided by length of the query protein

Name	Volume [Å³]	Surface [Å²]	Lipo surface [Å²]	Depth [Å]	Drug Score
P0SP0	821.70	981.81	507.72	0.51	0.50
P0SP1	547.28	692.27	409.86	0.00	0.29
P0SP2	492.99	653.04	334.33	22.78	0.24
P0SP3	350.73	402.70	247.82	0.72	0.24
P0SP4	334.92	574.86	303.45	10.63	0.16
P0SP5	180.87	412.00	240.74	8.39	0.12
P0SP6	141.87	282.39	125.94	10.23	0.08
P0SP7	118.94	335.00	230.86	7.89	0.23
P0SP8	78.52	278.20	144.61	6.48	0.08
P0SP9	69.45	198.43	156.17	4.91	0.35
P1SP0	772.72	1000.66	688.93	15.48	0.68
P1SP1	399.06	535.00	306.10	15.26	0.42
P1SP2	239.95	346.52	196.53	0.00	0.23
P1SP3	135.27	299.68	182.46	8.19	0.18
P2SP0	506.47	605.91	308.39	19.26	0.33
P2SP1	426.66	437.64	289.26	0.00	0.37
P2SP2	62.71	96.91	55.53	0.51	0.45
P2SP3	52.73	157.99	56.52	1.13	0.12
P3SP0	543.39	685.79	353.71	15.26	0.24
P3SP1	140.84	220.03	117.96	8.97	0.09
P3SP2	116.61	228.93	106.44	7.67	0.10
P3SP3	110.78	99.23	74.05	0.00	0.48
P6SP0	316.66	372.21	309.73	13.32	0.59
P6SP1	56.88	160.49	87.76	4.38	0.20
P7SP0	136.17	284.73	206.76	7.32	0.18
P7SP1	111.17	251.06	178.48	7.45	0.28
P7SP2	55.32	225.53	175.75	4.77	0.36
P8SP0	185.67	409.65	253.92	11.36	0.27
P8SP1	102.87	225.14	132.50	6.67	0.22
P9SP0	183.59	234.45	156.74	7.62	0.20
P9SP1	67.11	140.31	120.75	1.13	0.25
P10SP0	200.95	208.09	126.66	12.61	0.28
P10SP1	49.23	96.01	71.41	6.90	0.36
P14SP0	132.80	223.08	94.78	7.66	0.16
P14SP1	70.35	109.01	77.71	0.51	0.32
P15SP0	132.29	273.58	146.12	8.54	0.15
P15SP1	55.71	111.95	83.57	0.51	0.34
P16SP0	108.58	284.10	149.43	9.56	0.12
P16SP1	71.52	225.68	116.35	7.79	0.15
P17SP0	83.70	222.85	190.07	6.67	0.35
P17SP1	68.15	211.94	199.00	6.26	0.38

undruggable => druggable

Fig. 5: Subpocket descriptor

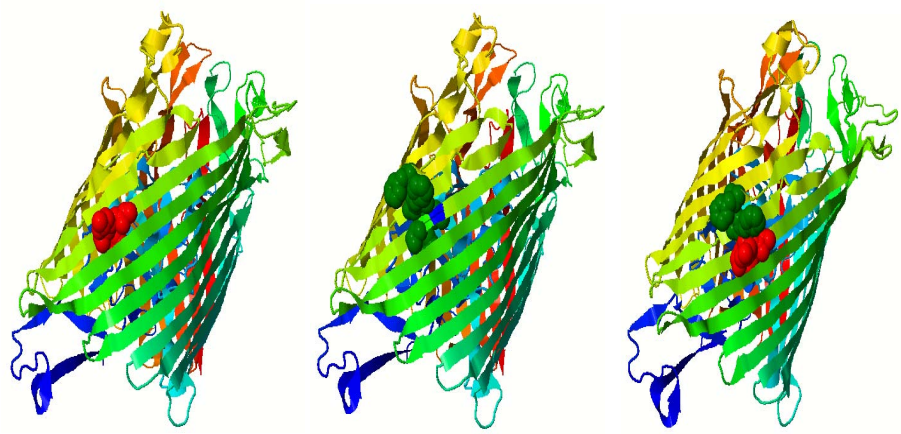

Fig. 6: Functional residues on FhuE 3D structure

CONCLUSION

Antibodies directed against these proteins associated with iron uptake exert a bacteriostatic or bactericidal effect by blocking siderophore mediated iron uptake pathways. The structural homology displayed by these receptors permits modelling of the 3D structure of Fhue in the absence of crystallographic data.

REFERENCES

Andrews, S.C., A.K. Robinson and F. Rodriguez-Quinones, 2003. Bacterial iron homeostasis. FEMS Microbiol. Rev., 27: 215-237.

Aydýn, M., M.T. Yavuz, O. Korkut and M. Oldacay, 2013. Antibiotic resistance profile of Acinetobacter strains isolated from patients in the intensive care unit: A surveillance study of four years. Mediterr. J. Infect. Microbes Antimicrobials, 2: 13-13.

Darbandian, P. and F. Sefid, 2017. Evaluation of OMP A (Outer Membrane Protein A) linear and conformational epitopes in *Acinetobacter baumannii*. Intl. J. Adv. Biotechnol. Res., 7: 994-1003.

Dehghani, E. and F. Sefid, 2016. Evaluation of lamb linear and conformational Epitopes on the *Vibrio harveyi*. Intl. J. Biol. Biotechnol., 7: 664-671.

Dijkshoorn, L., A. Nemec and H. Seifert, 2007. An increasing threat in hospitals: Multidrug-resistant *Acinetobacter baumannii*. Nat. Rev. Microbiol., 5: 939-951.

Eliopoulos, G.M., L.L. Maragakis and T.M. Perl, 2008. Acinetobacter baumannii: Epidemiology, antimicrobial resistance and treatment options. Clin. Infect. Dis., 46: 1254-1263.

Gaddy, J.A., B.A. Arivett, M.J. McConnell, L.R. Rojas and J. Pachon *et al*., 2012. Role of acinetobactin-mediated iron acquisition functions in the interaction of *Acinetobacter baumannii* strain ATCC 19606T with human lung epithelial cells, *Galleria mellonella* caterpillars and mice. Infect. Immun., 80: 1015-1024.

Ganz, T., 2009. Iron in innate immunity: Starve the invaders. Current Opinion Immunol., 21: 63-67.

Kafee, N. and F. Sefid, 2016. Functional exposed amino acids of OSPA as a candidate for lyme disease vaccine. Intl. J. Adv. Biotechnol. Res., 7: 957-966.

Krewulak, K.D. and H.J. Vogel, 2008. Structural biology of bacterial iron uptake. Bioch. Biophy. Acta., 1778: 1781-1804.

Masoumi, S. and F. Sefid, 2016. In silico determination and validation of FptA structure and ligand binding site as a vaccine candidate in *Pseudomonas aeruginosa*. Intl. J. Adv. Biotechnol. Res., 7: 1038-1045.

Mihara, K., T. Tanabe, Y. Yamakawa, T. Funahashi and H. Nakao *et al*., 2004. Identification and transcriptional organization of a gene cluster involved in biosynthesis and transport of acinetobactin, a siderophore produced by *Acinetobacter baumannii* ATCC 19606T. Microbiol., 150: 2587-2597.

Ong, S.T., J.Z.S. Ho, B. Ho and J.L. Ding, 2006. Iron-withholding strategy in innate immunity. Immunobiol., 211: 295-314.

Payandeh, Z.A.H.R., A.S.E.F. Kofeiti and F.A.T.E. Sefid, 2015. Nanobody structure analysis and determination of the functional conserve amino acid with bioinformatic tools. Natl Agronomique Institute Ltd, France.

Peleg, A.Y., H. Seifert and D.L. Paterson, 2008. *Acinetobacter baumannii*: Emergence of a successful pathogen. Clin. Microbiol. Rev., 21: 538-582.

Ratledge, C. and L.G. Dover, 2000. Iron metabolism in pathogenic bacteria. Ann. Rev. Microbiol., 54: 881-941.

Sandrini, S.M., R. Shergill, J. Woodward, R. Muralikuttan and R.D. Haigh *et al*., 2010. Elucidation of the mechanism by which catecholamine stress hormones liberate iron from the innate immune defense proteins transferrin and lactoferrin. J. Bacteriol., 192: 587-594.

Santander, J., G. Golden, S.Y. Wanda and R. Curtiss, 2012. Fur-regulated iron uptake system of *Edwardsiella ictaluri* and its influence on pathogenesis and immunogenicity in the catfish host. Infect. Immun., 80: 2689-2703.

Sefid, F., I. Rasooli and A. Jahangiri, 2013. In silico determination and validation of *Baumannii acinetobactin* utilization a structure and ligand binding site. BioMed Res. Intl., 2013: 1-14.

Sefid, F., I. Rasooli and Z. Payandeh, 2016. Homology modeling of a Camelid antibody fragment against a conserved region of *Acinetobacter baumannii* biofilm associated protein (Bap). J. Theor. Biol., 397: 43-51.

Sefid, F., I. Rasooli, A. Jahangiri and H. Bazmara, 2015. Functional exposed amino acids of BauA as potential ImmunoGen against *Acinetobacter baumannii*. Acta Biotheor., 63: 129-149.

Skaar, E.P., 2010. The battle for iron between bacterial pathogens and their vertebrate hosts. PLoS Pathog, 6: 1-4.

Valencia, R., L.A. Arroyo, M. Conde, J.M. Aldana and M.J. Torres *et al*., 2009. Nosocomial outbreak of infection with pan-drug-resistant *Acinetobacter baumannii* in a tertiary care university hospital. Infect. Control Hosp. Epidemiol., 30: 257-263.

Vallenet, D., P. Nordmann, V. Barbe, L. Poirel and S. Mangenot *et al*., 2008. Comparative analysis of Acinetobacters: Three genomes for three lifestyles. PloS One, 3: 1-11.

Zimbler, D.L., B.A. Arivett, A.C. Beckett, S.M. Menke and L.A. Actis, 2013. Functional features of TonB energy transduction systems of *Acinetobacter baumannii*. Infect. Immun., 81: 3382-3394.

Zimbler, D.L., W.F. Penwell, J.A. Gaddy, S.M. Menke and A.P. Tomaras *et al*., 2009. Iron acquisition functions expressed by the human pathogen *Acinetobacter baumannii*. Biometals, 22: 23-32.